

Intramolecular Charge-Transfer Mechanism in Quinolidines: The Role of the Amino Twist Angle

Christof Hättig,^{†,||} Arnim Hellweg,^{‡,||} and Andreas Köhn^{*,§,⊥}

Contribution from the Forschungszentrum Karlsruhe, Institute of Nanotechnology, P.O. Box 3640, D-76021 Karlsruhe, Germany, Institut für Physikalische Chemie, Universität Karlsruhe (TH), D-76128 Karlsruhe, Germany, and Center for Theoretical Chemistry, Department of Chemistry, Århus University, DK-8000 Århus, Denmark

Received June 14, 2006; E-mail: andreas.koehn@uni-mainz.de

Abstract: Quantum-chemical calculations with the approximate coupled-cluster singles-and-doubles model CC2 have been carried out for 1-*tert*-butyl-6-cyano-1,2,3,4-tetrahydroquinoline (NTC6). For this molecule dual fluorescence was experimentally observed, raising the discussion about the importance of the amino twist angle for this process. The calculations suggest that both the ground state and the normal fluorescent state are significantly twisted by 30°–40° and that the molecule is flexible enough to move into an even stronger twisted conformation (60°–70°) in its intramolecular charge-transfer (ICT) state which is responsible for the anomalous fluorescence band. Such a conformation both minimizes the total energy in the S₁ state and maximizes the dipole moment. The barrier from the normal fluorescent state to the ICT state region is very small. Comparison to the situation in the 1-methyl-derivative NMC6 suggests that a large alkyl substituent makes the preferably planar normal fluorescent state energetically unfavorable compared to the ICT state and thus promotes the occurrence of dual fluorescence.

1. Introduction

Intramolecular charge-transfer (ICT) states play a key role for the phenomenon of dual fluorescence. The model molecule showing dual fluorescence is 4-(*N,N*-dimethylamino)benzonitrile (DMABN) for which, apart from a fluorescence band in the energy region expected for this kind of molecules and ascribed to a so-called locally excited (LE) state, a second, strongly red-shifted emission band can be observed.^{1–4} It is now well-established that this “anomalous” fluorescence is due to a highly polar intramolecular charge-transfer (ICT) state. However, the structure of the latter is still a subject of some controversy.^{4–9}

Basically, there is disagreement whether a strong twist of the amino group (or in general: the donor group) with respect to the plane of the phenyl group (in general: the acceptor group)

is a necessary condition for the formation of a fluorescent ICT state or not. The twisted ICT (TICT) hypothesis¹⁰ postulates such a twist as a consequence of an electron transfer from the amino group to the phenyl group which results in a biradicalic structure of singlet spin symmetry, with one electron occupying a π^* orbital of the acceptor group and the other remaining in the nitrogen lone-pair orbital. In a simple orbital model such a singlet-coupled electronic structure can lower its energy by minimizing the overlap between the two orbitals which the unpaired electron occupies, the “minimum-overlap principle”.² The thus induced energy lowering is thought to be responsible for the formation of an energetically low-lying ICT state. Consequently a sufficient flexibility of the molecule is expected to be a prerequisite for the observation of fluorescence out of an ICT state.

The so-called planar ICT (PICT)⁶ model denies the necessity of such a large-amplitude motion for the formation of a highly polar ICT state, as the equilibration dynamics between the LE and ICT state take place on a picosecond scale with increasing rates for larger alkyl substituents on the amino group.³ The PICT model postulates an ICT structure with an increased double bond character between the amino-group nitrogen and the phenyl group (denoted the Ph–N bond hereafter), resulting in a partial positive charge on the amino group and a quinone-like structure of the phenyl-ring. In a more general interpretation of the model, it is claimed that the only important condition for the occurrence of ICT is a small energy gap between S₁ and S₂ in the Franck–Condon region, whereas, with respect to the structure, it is only

[†] Forschungszentrum Karlsruhe.

[‡] Universität Karlsruhe (TH).

[§] Århus University.

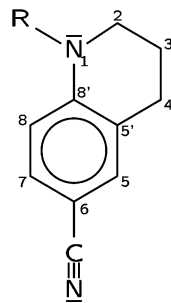
^{||} New address: Lehrstuhl für Theoretische Chemie, Ruhr-Universität Bochum, D-44780 Bochum, Germany.

[⊥] New address: Institut für Physikalische Chemie, Universität Mainz, D-55099 Mainz, Germany.

- (1) Lippert, E.; Lüder, W.; Boos, H. In *Advances in Molecular Spectroscopy*; Mangini, A., Ed.; Pergamon: Oxford, 1962; pp 443–457.
- (2) Rettig, W. *Angew. Chem., Int. Ed. Engl.* **1986**, *25*, 971–988.
- (3) Zachariasse, K. A.; von der Haar, T.; Hebecker, A.; Leinhos, U.; Kühnle, W. *Pure Appl. Chem.* **1993**, *65*, 1745–1750.
- (4) Grabowski, Z. R.; Rotkiewicz, K.; Rettig, W. *Chem. Rev.* **2003**, *103*, 3899–4031.
- (5) Rettig, W.; Bliss, B.; Dimberger, K. *Chem. Phys. Lett.* **1999**, *305*, 8–14.
- (6) Zachariasse, K. A. *Chem. Phys. Lett.* **2000**, *320*, 8–13.
- (7) Zachariasse, K. A.; Druzhinin, S. I.; Bosch, W.; Machinek, R. *J. Am. Chem. Soc.* **2004**, *126*, 1705–1715.
- (8) Techert S.; Zachariasse, K. A. *J. Am. Chem. Soc.* **2004**, *126*, 5593–5600.
- (9) Yoshihara, T.; Druzhinin, S. I.; Zachariasse, K. A. *J. Am. Chem. Soc.* **2004**, *126*, 8535–8539.

- (10) Grabowski, Z. R.; Rotkiewicz, K.; Siemiarz, A.; Cowley, D. J.; Baumann, W. *Nouv. J. Chim.* **1979**, *3*, 443–454.

Scheme 1



stated that a strong (or even (near-)perpendicular) twist is not necessary to form a highly polar ICT state.⁷

For DMABN, time-resolved vibrational spectra¹¹ in concert with theoretical calculations^{12–14} give strong support to a biradicalic electronic structure (most likely resulting in a TICT conformation) as the measured modes are consistent with a weakened Ph–N bond. Recent experiments, however, raised doubts about the role of the amino group twist in the dual fluorescence mechanism,^{7–9} even within the rather restricted group of alkyl-aminobenzonitriles.¹⁵

A recent time-resolved X-ray diffraction⁸ experiment suggests that in crystalline 4-(*N,N*-diisopropylamino)benzotrile (DIABN) the excited state (10° amino twist angle) is more planar than it is in the ground state (14°). This finding is in conflict with the assumption of a biradicalic ICT state for which an increased twist angle is expected even though a large twist angle may be prevented by packing effects.

The present work has, however, been motivated by recent experimental results where dual fluorescence was observed for 1-*tert*-butyl-6-cyano-1,2,3,4-tetrahydroquinoline (NTC6; Scheme 1, R = *t*Bu),⁷ in which the twist motion of the amino group was supposed to be sterically hindered. This observation was particularly amazing as the absence of dual fluorescence for the 1-methyl and 1-ethyl derivatives (NMC6 and NEC6) was one of the main experimental arguments in favor of the TICT hypothesis.⁴ Therefore we investigated the systems NMC6 and NTC6, using the second-order approximate coupled-cluster singles and doubles model CC2¹⁶ in connection with high-level basis sets. The model was previously successfully applied to DMABN and calibrated by comparison to more advanced coupled-cluster models.¹⁴ In this work, we employed a parallelized version of the RI-CC2 code^{17–19} which made the current application feasible.

After giving a survey of the employed computational methods, section 2, we will in section 3 successively present the structures of the ground state, the LE state, and the ICT state of NMC6 and NTC6, including a comparison to DMABN. The discussion of the LE state also includes the *iso*-propyl-derivative NIC6; see section 3.2. The reason for the occurrence

of dual fluorescence in NTC6 and for its absence in NMC6 will be discussed in section 3.4. A summary and final conclusions are given in the last section.

2. Computational Procedure

All computations were carried out with the analytical gradient code for RI-CC2,^{17,18,20} which is part of the TURBOMOLE suite of programs.²¹ CC2 is a second-order approximation to the coupled-cluster singles-and-doubles (CCSD) model¹⁶ and can be favorably implemented using the resolution of the identity (RI) approximation^{22–24} for fast evaluation of the electron repulsion integrals.¹⁷ Excited-state energies and properties are calculated by applying the coupled-cluster response theory. A recently developed parallelized version¹⁹ of the program was used to efficiently treat molecules of the present size and complexity.

For an account of the capabilities and the restrictions of the CC2 model, the reader is referred to refs 18, 20. Here, we only note that CC2 provides for vertical excitation energies a slightly better accuracy than the perturbative doubles correction to configuration interaction singles²⁵ (CIS(D)) and that CC2 can be applied for the optimization of excited states even in the vicinity of avoided crossings, in contrast to CIS(D) which relies on a nondegenerate perturbation theory. In ref 14 the model was applied to DMABN, the “root” derivative of NMC6 and NTC6. In the latter article, CC2 results were compared with single-point calculations using more elaborate coupled-cluster models and with relaxed structures obtained from CASSCF. These tests appeared necessary as the impact of double excitations was significant for DMABN, their contributions to the biorthogonal norm of the excitation vector amounting to 10–15%. The calculations confirmed the CC2 results, in particular the (somewhat unexpected) out-of-plane bend of the amino group. The characters of the excited states are very similar for NMC6 and NTC6, with similar biorthogonal norms, and we expect that the accuracy of CC2 established for DMABN carries over to these systems.

For the optimization of the equilibrium structures, high quality basis sets of triple- ξ quality (TZVPP, refs 26, 27) were employed in connection with optimized auxiliary basis sets for the RI approximation.²⁷ For NTC6 the one-electron and auxiliary basis sets comprised of, respectively, 748 and 1756 basis functions, and for NMC6 of, respectively, 571 and 1348 basis functions. The 1s² cores of the carbon and nitrogen atoms were kept frozen in the correlation treatment. For the minimum energy path calculations a more economic basis set of double- ξ quality (split valence: SVP, ref 28) was chosen.

The geometries of the ground and excited states were fully optimized using standard optimization techniques based on analytic gradients. Because of the conformational flexibility of the aliphatic bridge and the substituent R (i.e., Me or *t*Bu) the potential energy surfaces of NMC6 and NTC6 feature several local minima which are almost degenerate in energy. For the excited states the searches for the equilibrium structures were started from vertical excitations at the minima of the electronic ground state. The structures found this way are not necessarily the global minima on the excited-state surfaces but are likely those which can most easily and rapidly be reached after an excitation out of the electronic ground state; i.e., these structures are

- (11) Kwok, W. M.; Ma, C.; Matousek, P.; Parker, A. W.; Phillips, D.; Toner, W. T.; Towrie, M.; Umapathy, S. *J. Phys. Chem. A* **2001**, *105*, 984–990.
- (12) Dreyer, J.; Kummrow, A. *J. Am. Chem. Soc.* **2000**, *122*, 2577–2585.
- (13) Rappoport, D.; Furche, F. *J. Am. Chem. Soc.* **2004**, *126*, 1277–1284.
- (14) Köhn A.; Hättig, C. *J. Am. Chem. Soc.* **2004**, *126*, 7399–7410.
- (15) Thereby we exclude any derivatives with substituents that introduce further low-lying states into the spectrum, such as phenyl-pyrroles like fluorazene (FPP). For this molecule, dual fluorescence was observed, as well (ref 9).
- (16) Christiansen, O.; Koch, H.; Jørgensen, P. *Chem. Phys. Lett.* **1995**, *243*, 409–418.
- (17) Hättig C.; Weigend, F. *J. Chem. Phys.* **2000**, *113*, 5154–5162.
- (18) Köhn A.; Hättig, C. *J. Chem. Phys.* **2003**, *119*, 5021–5036.
- (19) Hättig, C.; Hellweg, A.; Köhn, A. *Phys. Chem. Chem. Phys.* **2006**, *8*, 1159–1169.

- (20) Hättig, C. *J. Chem. Phys.* **2003**, *118*, 7751–7761.
- (21) Ahlrichs, R.; Bär, M.; Horn, H.; Kölmel, Ch. *Chem. Phys. Lett.* **1989**, *162*, 165–169.
- (22) Whitten, J. L. *J. Chem. Phys.* **1973**, *58*, 4496–4501.
- (23) Dunlap, B. I.; Conolly, J. W. D.; Sabin, J. R. *J. Chem. Phys.* **1979**, *71*, 3396–3402.
- (24) Vahtras, O.; Almlöf, J. E.; Feyereisen, M. W. *Chem. Phys. Lett.* **1993**, *213*, 514–518.
- (25) Head-Gordon, M.; Rico, R. J.; Oumi, M.; Lee, T. J. *Chem. Phys. Lett.* **1994**, *219*, 21–29.
- (26) Schäfer, A.; Huber, C.; Ahlrichs, R. *J. Chem. Phys.* **1994**, *100* (8), 5829–5835.
- (27) Weigend, F.; Häser, M.; Patzelt, H.; Ahlrichs, R. *Chem. Phys. Lett.* **1998**, *294*, 143–152.

Table 1. Calculated Absorption and Emission Energies and Dipole Moments for DMABN, NMC6, and NTC6 in Comparison with Experimental Data^a

	DMABN		NMC6		NTC6	
	CC2 ^b	expmt	CC2	expmt	CC2	expmt
absorption (S ₁) [eV]	4.41 ^c	4.25 ^d	4.31 ^e		4.33 ^e	
absorption (S ₂) [eV]	4.77 ^c	4.56 ^d	4.58 ^e	4.32 ^f	4.43 ^e	4.14 ^f
osc. strengths (S ₁)	0.03 ^{c,g}		0.03 ^g		0.03 ^g	
osc. strengths (S ₂)	0.62 ^{c,g}		0.49 ^g		0.51 ^g	
T _e (LE) [eV]	4.14		4.07		3.91	
emission (LE) [eV]	3.78 ^h	3.76 ⁱ	3.67 ^h	3.67 ^f	3.34 ^h	3.50 ^f
T _e (ICT) [eV]	4.06, 4.16 ^j		4.18		3.71	
emission (ICT) [eV]	2.49, 3.27 ^{h,j}	2.8–3.2 ^k	2.53 ^{h,l}		2.51 ^{h,l} , 3.15 ^{h,l}	2.8 ⁿ –3.3 ^f
dipole (GS) [D]	7.4	6.6 ^k	7.5	6.8 ^o	7.7	6.8 ^o
dipole (LE) [D]	10.1	9.7 ^k	10.4	10.6 ^o	12.6	
dipole (ICT) [D]	13.3, 15.1 ^j	17 ± 1 ^k	12.7 ^l		13.5, ^l 14.7 ^m	17–19 ^o

^a The CC2 results for absorption and emission energies are vertical electronic transition energies; the dipole moments were calculated as analytic derivatives of the CC2 total energies. ^b From ref 14 unless indicated otherwise. ^c CC2/TZVPP (ref 33). ^d EELS band maximum (ref 34). ^e Vertical excitation energy. ^f Experimental band maximum in *n*-hexane (ref 7). ^g Oscillator strength for vertical electronic transition calculated at the CC2/TZVPP level in length gauge. ^h Vertical energy separation from ground state at the excited-state equilibrium structure. ⁱ Maximum of dispersed emission from jet-cooled DMABN (ref 35). ^j The first value is the result for the gas-phase equilibrium structure, and the second value is obtained at the C_{2v} symmetric saddle point (ref 14). ^k Emission energy from ICT state from maxima of fluorescence bands; ground state dipole moment derived from the dielectric constant and refractive index in 1,4-dioxane; and the excited-state dipole moments from time-resolved microwave conductivity measurements combining data obtained in cyclohexene, benzene, and 1,4-dioxane (ref 36). ^l Value refers to the ICT-3 conformer. ^m Value refers to calculations on the ICT-3 conformer where the pyramidalization angle at C_g was confined to zero (ICT-P0). ⁿ Experimental band maximum in methanol (ref 7). ^o Reference 7. Excited-state dipole moments were derived from the solvatochromic shift of the fluorescence maximum.

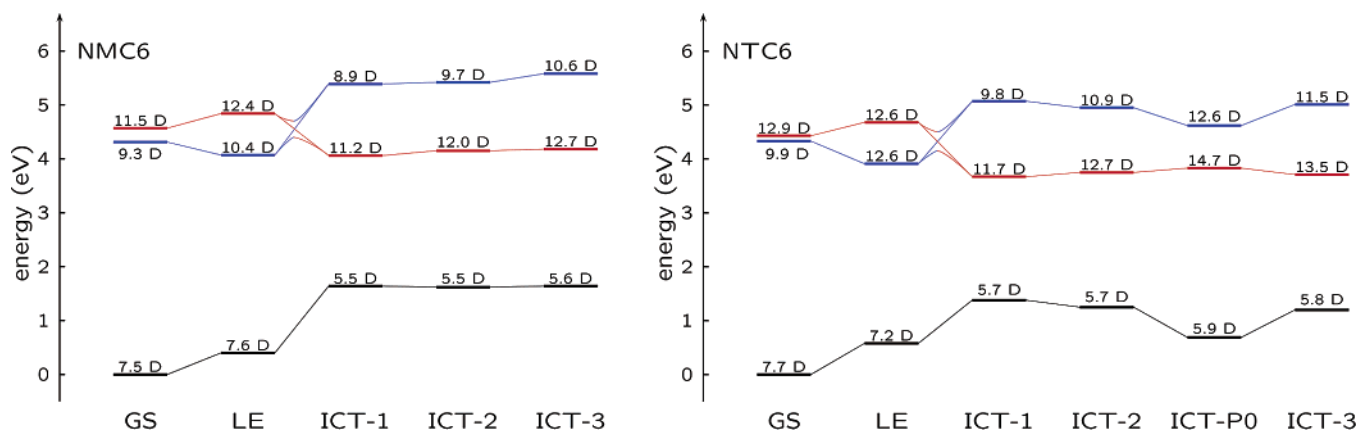


Figure 1. Energy diagrams for NMC6 (left) and NTC6 (right). Given are the calculated vertical energies (in eV) of S₀, S₁, and S₂ at the ground state (GS), the locally excited (LE) state, and the intramolecular charge transfer (ICT) state equilibrium geometries (all energies quoted relative to the ground state at its equilibrium geometry). The numbers on the bars give the calculated dipole moments (in Debye). The colors are chosen to visualize the similarity in the electronic structure of the S₂ state in the GS (i.e., Franck–Condon) and LE region and the S₁–ICT state. The different structures belonging to ICT-*n* (*n* = 1, 2, 3, P0) can be found in Figure 3. The ICT-P0 structure is the approximate transition structure between ICT-2 and ICT-3. It is also present for NMC6 but was not calculated for that molecule. Note that else the sequence of ICT structures is arbitrary and does not indicate which of these lies closer to the conical intersection indicated in the graphic.

most important for the short-time dynamics after excitation in the Franck–Condon region. Anyway, in an additional search for alternative conformational minima of the excited states we could not locate structures which were significantly lower in energy.

Due to the huge computational effort, no (numerical) force-constant calculations were carried out. Insofar we miss an unequivocal proof that all presented structures are indeed minima on the potential hypersurfaces. However, as none of the considered systems has an inherent spatial symmetry, it seems rather unlikely that any of the geometry optimizations resulted in a saddle point. This might only happen for internal coordinates that are connected with extremely low force constants such as methyl-group rotations. The small energy changes connected with such a coordinate, however, would not change any of the conclusions drawn in this work.

All presented calculations refer to isolated molecules in the gas phase. Therefore, a strict quantitative comparison to experiments carried out in solution is not possible. The treatment of solvent effects, however, is difficult in connection with coupled cluster theory, in particular for

electronically excited states. Therefore, solvent effects were estimated for some cases only, using a simple Onsager continuum approximation.^{29–32}

3. Results and Discussion

The following discussion refers to the numbering of atoms as given in Scheme 1. We will successively discuss the equilibrium structures calculated for the ground state, the LE state, and the ICT state. Table 1 gives an overview of the CC2/TZVPP results for some spectroscopic properties of NMC6 and NTC6, as the absorption and emission energies and the dipole moments, in comparison with results for DMABN and the available experimental data. Additionally, Figure 1 shows the

- (28) Schäfer, A.; Horn, H.; Ahlrichs, R. *J. Chem. Phys.* **1992**, *97* (4), 2571–2577.
- (29) Technical details of the model calculations are given in the Supporting Information.
- (30) Lippert, E. *Z. Naturforsch.* **1955**, *10a*, 541–545.
- (31) Majumdar, D.; Sen, R.; Bhattacharyya, K.; Bhattacharyya, S. P. *J. Phys. Chem.* **1991**, *95*, 4324–4329.
- (32) Parusel, A. B. *J. Phys. Chem. Chem. Phys.* **2000**, *2*, 5545–5552.

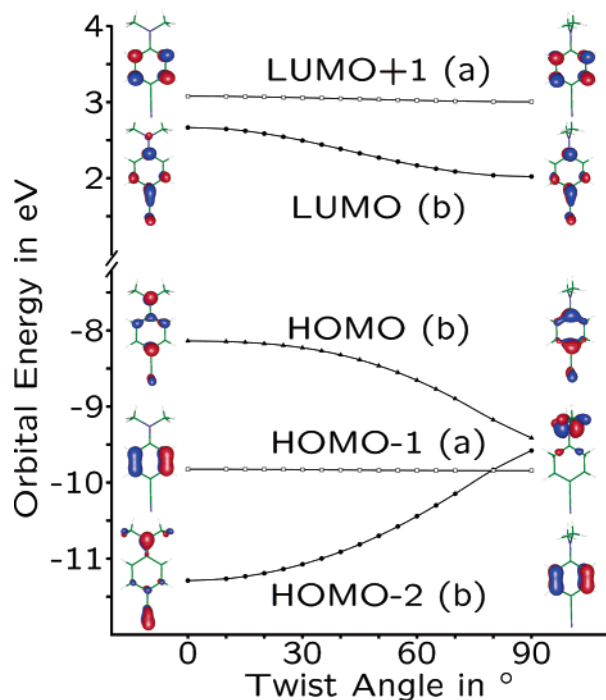


Figure 2. Frontier orbital of DMABN and their energies as function of the twist angle. The letter in parentheses specifies the irreducible representation of the orbital in point group C_2 .

vertical energy separations between the considered states of NMC6 and NTC6 for each structure.

As indicated in Figure 1, the LE and ICT minima can formally be attributed to two excited singlet hypersurfaces of different electronic characters which interchange as a function of some reaction coordinate going through a conical intersection. For DMABN this connection is established by the different irreducible representations of the LE (symmetry B) and ICT (symmetry A) state when C_2 point group symmetry is imposed. For the unsymmetrically substituted NMC6 and NTC6 symmetry cannot be used for that purpose, but for both molecules the excited states can still unequivocally be assigned by comparison of their electronic and geometric structures with those found for DMABN. The electronic structures of the S_1 and S_2 states in amino-benzonitriles can be rationalized in terms of the five frontier orbitals which are involved in the main contributions to the transitions into these states:³² the three highest occupied (HOMO-2, HOMO-1, and HOMO) and the two lowest unoccupied (LUMO and LUMO + 1) molecular orbitals in the ground state. These are depicted for DMABN in Figure 2 together with the respective orbital energies as a function of the twist angle calculated at the SCF/SVP level for an idealized C_2 -symmetric structure. The diagram will be used in the following sections to rationalize the observed structure changes in the excited states.

3.1. Ground State. The most striking feature is the rather small structural influence of the aliphatic ring in NMC6 and NTC6, as compared to DMABN. In particular for NMC6 and DMABN, we find basically identical structure constants, Table 2. Both molecules feature a pyramidalized amino group (described by the out-of-plane angle ϕ_1 , with values of 23° to 25°). The group is coplanar to the phenyl ring and the Ph-N bond is rather short, as compared to a typical C-N single bond, e.g., the bonds toward the alkyl groups in the amino moiety

Table 2. Calculated Bond Lengths (pm) and Angles (deg) of the Ground States of NMC6 and NTC6 in Comparison with the Results for DMABN

	DMABN	NMC6	NTC6
$d(C_8-N_1)$	137.7	138.1	139.0
$d(C_8-C_8')$	141.4	141.2	141.2
$d(C_8-C_5')$	141.4	141.9	141.1
$d(C_7-C_8)$	138.7	138.7	138.9
$d(C_5-C_5')$	138.7	138.9	138.6
$d(C_6-C_7)$	140.2	140.0	139.9
$d(C_5-C_6)$	140.2	140.2	140.3
$d(C_6-C_{CN})$	142.7	142.6	142.6
$d(CN)$	118.2	118.1	118.1
τ^a	0	0.1	27.9
ϕ_1^b	23	24.8	18.9
ϕ_2^c	<1	1	1.5

^a torsion angle, defined as the dihedral angle of the normals defined by the planes $C_8-C_8'-C_5'$ and $C_2-N_1-C_R$ and a vector pointing along the bond C_8-N_1 with respect to the plane defined by $C_2-N_1-C_R$ ("wagging" angle). ^b Out-of-plane angle of a vector pointing along the bond C_8-N_1 with respect to the plane defined by $C_2-N_1-C_R$ ("wagging" angle). ^c Out-of-plane angle of vector pointing along the bond C_8-N_1 with respect to the plane defined by $C_8-C_8'-C_5$.

(145 pm). This suggests a partial double bond character which is supported by the calculated Ph-N force constant of DMABN (see ref 14). The structural differences between NMC6 and NTC6 are induced by the sterically demanding *tert*-butyl substituent which makes a coplanar orientation unfavorable. Rather, a tilted geometry with a twist angle of about 28° (cf. Table 2) is found for NTC6. Amatatsu³⁷ reports twisted ground state structures for both NMC6 and NTC6, using Hartree-Fock and a nonstandard polarized double- ζ basis (see ref 37 for its definition). With the more advanced CC2 method, however, no twisted minimum structure for NMC6 could be reproduced.

Experimental structures are available for DMABN only (from X-ray diffraction, ref 38). These have been compared to the structure parameters calculated by CC2 in ref 14 which results in deviations of up to +1.5 pm for all bonds (except for the cyano triple bond, vide infra) which is in good agreement with experiment. As noted in ref 14, CC2 tends to predict somewhat too large bond lengths²⁰ which becomes most obvious for the triple bond of the cyano group which is 3.7 pm too long compared to that in the X-ray structure. This shortcoming of CC2 has been investigated before, and differential properties as adiabatic excitation energies and changes in the bond length upon excitation were shown to be much less affected.¹⁸

We note that calculations of the transition moments for the vertical excitations into S_1 and S_2 yield similar values for both species despite the different twist angles τ . This is in agreement with the experimental spectra⁷ but in contrast to the cosine-square law³⁹ which relates the oscillator strength f to the twist angle of anilines τ according to

$$f = f_0 \cos^2 \tau.$$

- (33) Köhn, A. Ph.D. thesis, Universität Karlsruhe, 2003.
 (34) Bulliard, C.; Allan, M.; Wirtz, G.; Haselbach, E.; Zachariasse, K. A.; Detzer, N.; Grimme, S. *J. Phys. Chem. A* **1999**, *103*, 7766–7772.
 (35) Lommtanzsch, U.; Gerlach, A.; Lahmann, Ch.; Brutschy, B. *J. Phys. Chem. A* **1998**, *102*, 6421–6435.
 (36) Schuddeboom, W.; Jonker, S. A.; Warman, J. M.; Leinhos, U.; Kühnle, W.; Zachariasse, K. A. *J. Phys. Chem.* **1992**, *96*, 10809–10819.
 (37) Amatatsu, Y. *J. Phys. Chem. A* **2005**, *109*, 7225–7235.
 (38) Heine, A.; Herbst-Irmer, R.; Stalke, D.; Kühnle, W.; Zachariasse, K. A. *Acta Crystallogr.* **1994**, *B50*, 363–373.
 (39) Kleven H. B.; Platt, J. R. *J. Am. Chem. Soc.* **1949**, *71*, 1714–1720.

Table 3. Calculated Bond Lengths (pm) and Angles (deg) for the Locally Excited States of NMC6 and NTC6 in Comparison with the Results for DMABN

	DMABN	NMC6	NTC6
$d(C_8N_1)$	138.8	139.0	142.1
$d(C_8C_8')$	141.6	143.2	145.0
$d(C_8C_5')$	141.6	140.4	138.4
$d(C_7C_8)$	143.6	141.9	140.1
$d(C_5C_5')$	143.6	144.8	144.4
$d(C_6C_7)$	141.3	140.8	139.9
$d(C_5C_6)$	141.3	141.6	143.6
$d(C_6CCN)$	142.6	142.5	142.0
$d(CN)$	118.3	118.3	118.5
τ^a	19	15.8	38.6
ϕ_1^a	0	2.2	9.0
ϕ_2^a	0	1.1	8.0

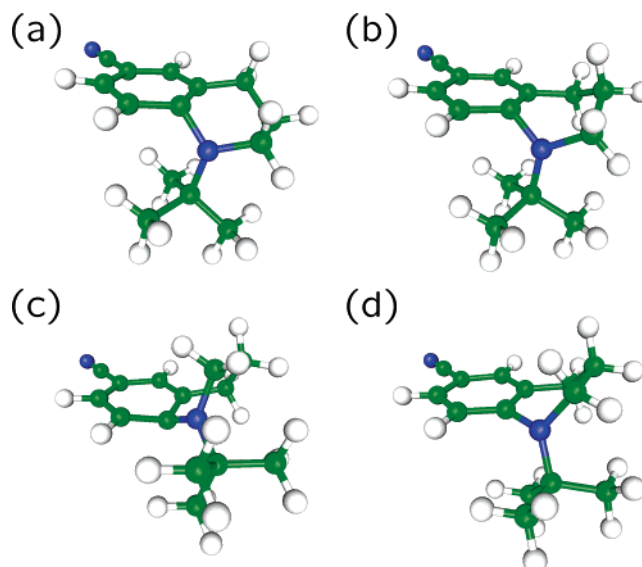
^a For the definition of the torsion and the out-of-plane angles, see Table 2.

Deviations from this relation have been observed earlier for amino-benzonitriles with strong donor–acceptor character.⁴⁰

3.2. Locally Excited State. As for the ground states, the sterical strain of the aliphatic bridge does not play a decisive role for the locally excited states of NMC6 and NTC6, even though the differences in the structures of DMABN, NMC6, and NTC6 are somewhat larger. This concerns in particular the bond pattern of the phenyl moiety which for NMC6 and NTC6 is not purely anti-quinoid, as this is the case for DMABN; see Table 3. Rather the unsymmetrical substitution leads to an additional Kekulé-type distortion which is most pronounced for NTC6.

In the Franck–Condon region the transition to the LE state (in this connection often referred to as L_b state) is dominated by the one-electron HOMO \rightarrow LUMO + 1 excitation (with a weight of about 85% in the CC2 excitation vector). While the HOMO is Ph–N antibonding, the LUMO + 1 is Ph–N nonbonding. From this very simple MO picture an even stronger Ph–N double bond character is expected. This is not completely the case, yet we observe a still rather short Ph–N bond; see Table 3. As the transition has a slight charge-transfer character and removes a part of the lone-pair electrons from nitrogen, the pyramidalization angle of the amino group becomes nearly zero. This effect increases the sterical strain between the alkyl groups on the amino moiety and the phenyl group and leads for all three systems to a slight twist of the amino group; see Table 3. The twist angle is very similar for DMABN (19°) and NMC6 (16°), whereas, due to the bulky *tert*-butyl substituent, NTC6 has a substantially larger twist angle of 39°. As a consequence, the LE state of NTC6 has a rather high dipole moment, but the long C₇–C₈ and C₅–C_{5'} bonds (cf. Table 3) distinguish this state clearly from the quinoidal ICT state structures. The assignment is further corroborated by the similarity of the frontier orbitals involved in the excitation at the equilibrium structure of the LE state.

The rather high dipole moment of the LE state of NTC6 is particularly astonishing as experiments suggest very similar excited-state dipole moments for the molecules NMC6, NEC6, and NIC6 (all of which do not show ICT fluorescence).⁷ Therefore, the locally excited state of NIC6 was optimized at the same level of theory as that for NMC6 and NTC6. The calculation resulted in a structure analogous to NMC6 with a

**Figure 3.** Equilibrium structures calculated at the CC2/TZVPP level for the ICT state of NTC6: (a) ICT-1, (b) ICT-2, and (c) ICT-3. (d) ICT-P0: Nonpyramidalized “transition structure” between ICT-2 and ICT-3 obtained by constraining the pyramidalization angle at C₈ to zero.**Table 4.** Calculated Bond Lengths (pm) and Angles (deg) and Weights of the Two Most Important One-Electron Excitations (%) for the Intramolecular Charge-Transfer States of NMC6 and NTC6 in Comparison with the Results for DMABN

	DMABN		NMC6			NTC6		
	ICT	ICT-1	ICT-2	ICT-3	ICT-1	ICT-2	ICT-3	
$d(C_8N_1)$	144.3	146.8	145.5	145.0	146.8	145.3	145.7	
$d(C_8C_8')$	144.6	143.5	143.7	144.8	142.9	143.1	144.9	
$d(C_8C_5')$	144.6	146.2	146.0	144.5	146.0	145.1	143.6	
$d(C_7C_8)$	137.2	137.2	137.0	137.7	137.3	137.2	137.8	
$d(C_5C_5')$	137.2	138.0	137.9	137.0	137.9	137.7	137.1	
$d(C_6C_7)$	142.9	143.4	143.7	142.5	143.8	144.1	142.4	
$d(C_5C_6)$	142.9	141.8	142.3	143.7	141.9	142.8	144.0	
$d(C_6CCN)$	140.9	141.2	141.0	141.0	141.1	140.8	140.8	
$d(CN)$	118.9	118.8	118.9	118.9	118.8	119.0	118.9	
τ^a	90	54.3	65.8	66.6	58.5	69.1	65.0	
ϕ_1^a	0	24.1	22.5	14.7	20.7	15.1	5.2	
ϕ_2^a	41	43.9	43.8	44.6	36.4	34.0	43.4	
HOMO \rightarrow LUMO		65	65	62	69	69	64	
HOMO–2 \rightarrow LUMO		15	15	17	25	22	16	

^a For the definition of the torsion and the out-of-plane angles, see Table 2.

dipole moment of 10.7 D, similar to that of the LE states of DMABN and NMC6. A closer inspection of the structures of NIC6 and NTC6 shows that there is a subtle balance between sterical interactions of the alkyl substituent with either the phenyl moiety or the aliphatic ring. Only in the case of NTC6, this enforces a larger twist of the amino group, resulting in a sudden increase of the dipole moment in the series NMC6, NEC6, NIC6, NTC6.

3.3. Intramolecular Charge-Transfer State. For both molecules NMC6 and NTC6, we found three ICT state conformations which are very close in energy; see Figure 1. The structures are denoted as ICT-1, ICT-2, and ICT-3, respectively. For the case of NTC6, they are shown in Figure 3; the topologies of the NMC6 structures are completely analogous. The calculated structure constants are summarized in Table 4, in comparison with the structure of the twisted ICT state of DMABN. As in the latter molecule also in NMC6 and NTC6 the ICT equilibrium geometries display marked quinoid

(40) Rettig, W.; Rotkiewicz, K.; Rubaszewska, W. *Spectrochim. Acta* **1984**, *40A*, 241–249.

distortions (i.e., short C_7-C_8 and $C_5-C_{8'}$ bonds) of the aromatic ring system. The main finding is, however, that the aromatic ring is no longer confined to planarity in the excited state. Rather, the carbon atom C_8 is pyramidalized, as it was observed before in calculations on DMABN.^{14,41} Based on this finding for DMABN, it had been conjectured previously¹⁴ that this additional flexibility of the phenyl ring may help to realize twisted structures in the ICT state of NTC6. Indeed, in the current calculations we find twist angles of the amino group of up to 69° . It will be shown below, however, that such a twist angle is energetically accessible without C_8 pyramidalization, as well.

The three ICT structures mainly differ in the direction of pyramidalization at carbon atom $C_{8'}$ and the conformation of the aliphatic ring. The energetically lowest-lying structure is in both cases ICT-1, cf. Figure 1, which realizes a nearly ideal chair conformation of the aliphatic six-member ring (Figure 3a). The amino twist angles of these conformations are 54° (NMC6) and 58° (NTC6), respectively. The structure ICT-2 can be derived from ICT-1 by folding up one corner of the six-member ring (atom C_3), Figure 3b, while the conformation ICT-3 results from ICT-2 by an inversion of the pyramidalization at atom C_8 . These structures possess markedly higher amino twist angles than those for ICT-1, $65^\circ-69^\circ$ (see Table 4). For NMC6, both the ICT-2 and ICT-3 conformers are destabilized by more than 0.1 eV with respect to ICT-1. This energy increase is much lower for NTC6, where in particular the ICT-3 conformer lies at only 0.04 eV higher energy.

A fourth structure in the ICT region was optimized for NTC6 by constraining the $C_{8'}$ pyramidalization angle to zero, denoted as ICT-P0. This corresponds to an approximate transition structure between ICT-2 and ICT-3 (note that the exact transition structure needs not have a zero pyramidalization angle). It is only 0.12 eV higher in energy than the ICT-3 conformation and has the same large amino twist angle as the ICT-2 conformation (69°).

A strictly planar structure as originally proposed for the PICT state⁶ was not found. In the case of DMABN, even for a structure confined to C_{2v} symmetry we obtained a biradicalic electronic structure with a long Ph–N bond.¹⁴ This is in contrast to CASSCF optimizations that indeed find a PICT structure.^{12,41} Whether this difference is due to an artifact of either CC2 (which treats double excitation contributions only perturbatively) or CASSCF (which needs to compromise with the size of the active spaces) remains to be clarified. But it should be noted that irrespective of this, the PICT state found in CASSCF is always located on the S_2 surface at a markedly higher energy than the LE and the TICT state.^{12,41} It remains therefore doubtful that this particular structure plays an important role for the photo-physics of alkyl-aminobenzonitriles.

One reason for expecting a PICT state with a strongly conjugated amino group comes from the fact that the vertical transition to the S_2 state of DMABN (also referred to as transition to the L_a state) is dominated by the one-electron HOMO \rightarrow LUMO excitation, where the HOMO has Ph–N antibonding character. But actually, the LUMO has a Ph–N antibonding character as well and its orbital energy decreases slightly faster with increasing twist angle than the energy of

the HOMO; see Figure 2. Thus, already this simple model predicts that the ICT state has close to the ground state geometry a gradient directed toward a twisted structure.

With a growing twist angle the HOMO–2 \rightarrow LUMO excitation increasingly contributes to the transition. The HOMO–2 is the Ph–N binding counterpart of the HOMO. It rises in energy with τ and mixes with the HOMO. As τ approaches 90° one of the two orbitals becomes the lone pair at the amino nitrogen atom, while the other is localized in the aromatic system (minimum-overlap principle, ref 2) and the transition to the ICT state is dominated by the $n \rightarrow \pi^*$ excitation. In a many electron picture this change in the character of the excitation corresponds to an avoided crossing of the L_a state with a charge-transfer state which at the ground state structure lies above S_2 , according to the DFT/SCI calculation of ref 42 the S_5 or $3 A_1$ state. The avoided crossing with this state is the main driving force for the formation of the TICT structures (twist and pyramidalization at $C_{8'}$) in DMABN and other alkyl-substituted amino-benzonitriles. It leads to a pronounced stabilization of the ICT state at large twist angles and enhances the charge-transfer character, as it is apparent from the expectation values for the dipole moment (see Figure 1, and also Figure 2 of ref 14). For NMC6 and NTC6 we find a similar change in the electronic character from the vertical excitations to the L_a states in the Franck–Condon region which are, as in DMABN, dominated by the one-electron excitation out of the Ph–N antibonding HOMO, to the transitions at the ICT equilibrium geometries.

Since the twist in NTC6 and NMC6 is incomplete, the electronic structure at the equilibrium ICT geometries corresponds to an intermediate situation in the diagram shown in Figure 2. For both molecules, we find sizable contributions of the HOMO–2 \rightarrow LUMO excitations (with weights of about 15–25%) and furthermore the HOMOs have already assumed a perceptible N-lone-pair character as can be seen in Figure 4.

This probably also explains the trends seen in the dipole moment of the ICT state when going from DMABN to NTC6 and NMC6, since it follows from the character of the involved frontier orbitals that the dipole moment will increase with the twist angle τ . On the other hand, the pyramidalization at the carbon atom carrying the amino group ($C_{8'}$) goes together with a localization of the negative partial charge of the aromatic ring at this atom and thus a decrease of the dipole moment, as shown in ref 14. At the CC2/TZVPP level, the dipole moment of the ICT state in DMABN was obtained as 15.1 D for the C_{2v} symmetric saddle point, with the amino group twisted by 90° and a planar phenyl ring, while 13.1 D were found for the equilibrium geometries with pyramidalization at the $C_{8'}$ atom. All structures obtained for the ICT states of NMC6 and NTC6 feature a charge localization, and consequently we obtain dipole moments of 11.2–12.7 D and 11.7–13.5 D, respectively. The lower dipole moment of ICT-1 (as compared to ICT-2 and ICT-3) is obviously governed by the lower twist angle. The difference between the dipole moments of ICT-2 and ICT-3, however, seems to correlate with the degree of pyramidalization at N_1 (angle ϕ_1). For NTC6, we tested the effect of constraining ϕ_2 to zero (ICT-P0 structure), thereby suppressing the charge localization at $C_{8'}$. In fact, a high dipole moment of 14.7 D results, which is comparable to the situation in DMABN.

According to the Onsager model, the increase in the dipole moment by 1.2 D, going from ICT-3 to ICT-P0, results in an

(41) Gómez, I.; Reguero, M.; Boggio-Pasqua, M.; Robb, M. A. *J. Am. Chem. Soc.* **2005**, *127*, 7119–7129.

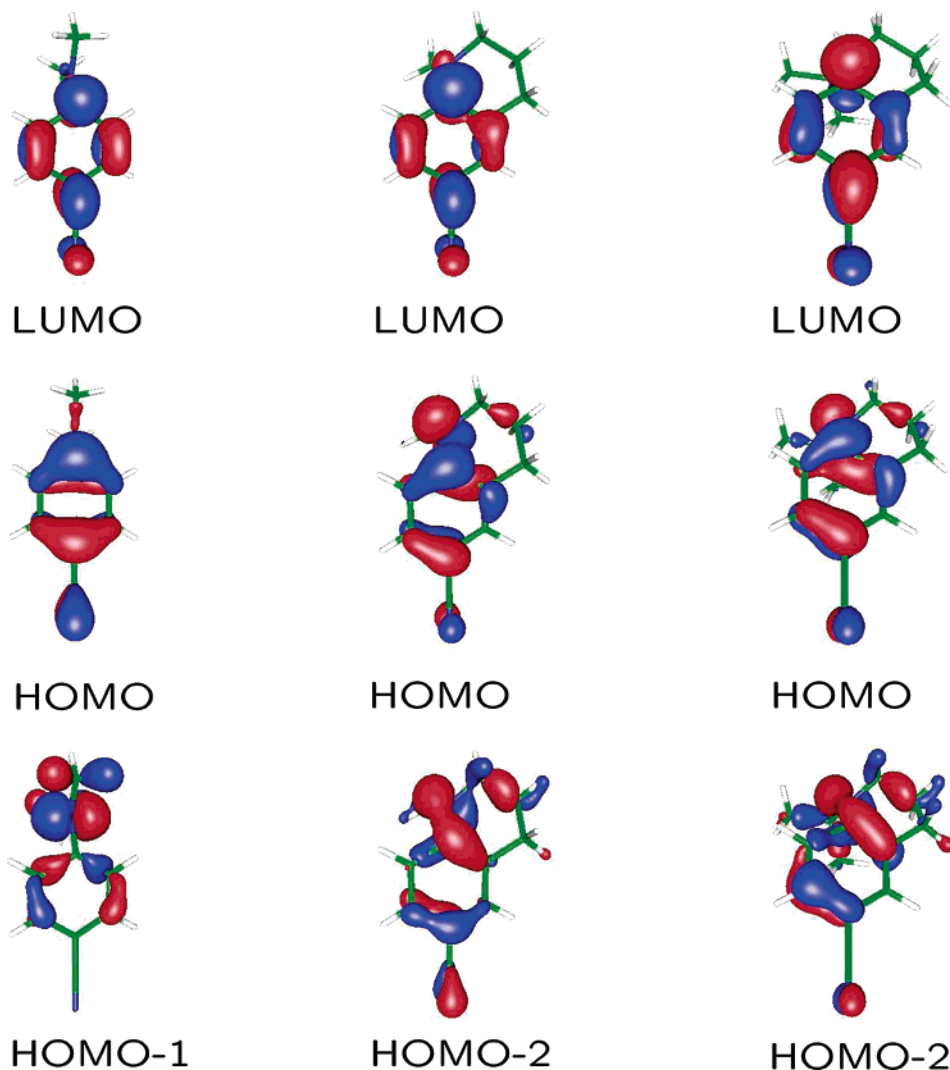


Figure 4. Frontier orbitals of NMC6 (middle column) and NTC6 (right column) at the equilibrium geometry of the intramolecular charge-transfer state (ICT-1 conformers) in comparison with the frontier orbitals of DMABN (left column).

additional solvation energy of 0.08 eV (*n*-hexane) to 0.11 eV (acetonitrile, even 0.2 eV if full solvent relaxation is assumed); i.e., in all solvents a significant shift of the ICT equilibrium toward the ICT-P0 structure can be expected. Similarly, this structure will become more favorable than the ICT-1 structure which has a 3 D lower dipole moment. The estimated solvent stabilization of ICT-P0 with respect to ICT-1 is 0.17 to 0.24 eV, which makes it likely that solvent effects compensate the in vacuo energy difference of 0.16 eV.

A fit to the solvatochromic shifts of the band maxima in fluorescence spectra reported in ref 7 indicates for NTC6 a strong dipole moment of 19 D in the ICT state, somewhat higher than that established for DMABN (17 D).³⁶ From the calculated values (13.5 to 14.7 D for NTC6 and 13.1 to 15.1 D for DMABN), on the other hand, it is expected that both molecules have about the same dipole moment. Yet, when comparing the calculated values with those from the experiment, it should be considered that the experimentally derived excited-state dipole moments are *effective* dipole moments of solvated molecules. They are obtained as parameters from approximate models (molecule assumed as rigid point dipole) for either microwave conductance or solvent shifts. The calculated dipole moments, on the other hand, refer to isolated molecules, and test

calculations on DMABN show that, e.g., electronic polarizability effects may increase the dipole moment by 1 to 2 D as soon as the reaction field from a solvent (even *n*-hexane) is present. Whether the observed solvatochromic shifts for NTC6 indeed translate into a stronger static in vacuo dipole moment of that molecule can only be assessed from more advanced solvation models and is beyond the scope of the present work. However, there is clear evidence from calculations that twisted structures enhance the excited-state dipole moment (see also refs 12–14, 42), such that the difference between experimental and calculated dipole moments does not indicate that other states different from the ones considered are involved.

Another feature connected with the C_8 pyramidalization angle ϕ_2 is the strong dependence of the energy gap between ICT and ground state on this coordinate. For low values of ϕ_2 , i.e., for the ICT-P0 structure, a vertical emission energy of 3.1 eV is found, whereas the gap for, e.g., the ICT-3 structure is only 2.5 eV (see Table 1 and Figure 1). The experimental value for the fluorescence maximum is 3.3 eV in *n*-hexane which could be best explained by assuming an ICT equilibrium structure close to ICT-P0. This interpretation is supported by the above estimates of the solvent stabilization energy. It should be noted, however, that the excited-state energy surface has a very shallow

minimum for ϕ_2 , whereas this is not the case for the ground state surface. This makes a prediction of the emission maximum difficult for two reasons: First, small errors in the excited-state energy surface (as compared to more accurate methods) may lead to large errors in the geometry which in turn results in relatively large errors for the vertical energy gap. And second, a shallow excited-state potential with considerable anharmonicity (as we are on one branch of a double minimum around $\phi_2 \approx 0$) implies a broad vibrational wavefunction that is not centered at the energetic minimum. This means that the emission maximum does not need to coincide with the vertical energy gap at the minimum structure of the excited state.

3.4. Dual Fluorescence of NTC6. So far, we have established that both NMC6 and NTC6 can potentially form a twisted ICT state, in the sense that the state has a biradicalic electronic structure which is stabilized by a twist of the amino group, as explained in the introduction. Yet, it remains to be understood why NTC6 is dually fluorescent while NMC6 is not. Certainly, the accuracy of the present calculations does not allow determination, a priori, which molecules are dually fluorescent and which are not, as the kinetics of the LE \rightarrow ICT reaction are very sensitive to the finer details of the potential energy surface. However, the comparison of calculations on DMABN, NMC6, and NTC6 gives clear hints that enable understanding the differences between these systems.

For the transition state between the LE and the (twisted) ICT minimum of DMABN an estimate of 0.1 eV (with respect to the LE minimum) was given in ref 14, based on a few exploratory calculations along the C_1 reaction path. Gómez and co-workers⁴¹ optimized the transition state structure at the state-averaged CASSCF level and calculated a barrier height of 0.78 eV (with respect to the LE minimum). However, the CASSCF calculations treat electron correlation only for the π -system and thus are not reliable for energy differences between structures that involve strong changes in the σ -system (note the large differences in the CASSCF, RASSCF, and CASPT2 energetics for the transition structure in the case of ABN in the same reference). In addition, we note that the transition structure reported in ref 41 features a strong pyramidalization of the ring carbon atom adjacent to the amino group which differs qualitatively from the transition structures obtained in our work which are much less pyramidalized (see below).

The reaction paths for NMC6 and NTC6 were investigated by constraining selected internal coordinates to fixed values and optimizing the remaining ones. A small SVP basis was used for cost effectiveness. As a reaction coordinate, a linear combination of the two dihedral angles defined by the atoms $C_8-C_8'-N_1-C_2$ and $C_5'-C_8'-N_1-C_R$ (compare Scheme 1) was used. To a good approximation this has the same effect as restricting the twist coordinate (defined above) which was not possible in the current implementation of the optimization program.

For both NMC6 and NTC6, the respective LE equilibrium structures were used as the starting point. Increasing the torsion angle leads to a raise in the total energy (see Figures 5 and 6) until an angle of 49° (NMC6) to 52° (NTC6) is reached, where a sudden decrease in the energy is found, accompanied by a strong structural change including both the C_8' pyramidalization and the formation of a quinoid bond pattern in the phenyl ring. Obviously, the torsional motion of the amino group is not a

good reaction coordinate in this region. Therefore the pyramidalization coordinate, given by the out-of-plane angle ϕ_2 as defined before, was additionally considered. Note that in the sign convention used for this figure a positive value for ϕ_2 implies a structural change toward ICT-3 (i.e., amino group above the phenyl plane in Figure 3), while a negative value means that we approach ICT-1/ICT-2 (amino group below the plane).

For the 40° amino-group torsion, the LE-like structures are still (at least local) minima with respect to ϕ_2 ; see Figures 5 and 6. In the case of NMC6, only a small barrier remains for negative ϕ_2 , while toward the ICT-3 region still a significant energy increase is found. At the 50° torsion angle the minimum at $\phi \approx 0$ has vanished, and the slope suggests that coming from the LE region of the hypersurface the molecule will preferably relax toward the ICT-1/ICT-2 region.

NTC6 differs clearly in this respect, as already for the 40° torsion for both directions (positive and negative ϕ_2) only small barriers are present; see Figure 6. At 51°, the LE-type minimum becomes a saddle point with respect to ϕ_2 , allowing for relaxation toward both ICT-1/ICT-2 and ICT-3. The trends in the dipole moments in the upper right panel suggest that solvation effects may favor trajectories toward ICT-3.

For NTC6, the barrier height along the considered reaction path is at most 0.04 eV (4 kJ/mol) with respect to the LE minimum. A single-point calculation at the highest energy point using a large TZVPP basis results in a barrier height of 8 kJ/mol, which confirms that the energetics will not change significantly upon enlarging the basis set. For NMC6, a barrier height of at least 0.12 eV results, corresponding to the lowest calculated energy point from which the system can relax into the ICT-1 region. The barrier toward ICT-3 is obviously higher in agreement with the fact that ICT-3 is located at 0.1 eV higher energy than the ICT-1 structure.

Comparing NMC6 and NTC6, we note that relative to a structure with a torsion angle of 40° both species possess low barriers toward the ICT region, around 0.02 eV for NMC6 (see Figure 5) and around 0.04 eV for NTC6 (see Figure 6). The main difference between both systems comes from the fact that NMC6 can further relax toward the LE region by around 0.08 eV (the equilibrium structure is at torsion angles of around 10° at the SVP level, whereas it was 16° at the TZVPP level). For NTC6, such a structure with a low amino twist angle is prevented by the bulky *tert*-butyl group (vide infra). In summary, the calculations indicate that no significant barrier hinders an equilibration reaction between the LE state and the partially twisted ICT states which we discussed in section 3.3.

We now turn to a discussion of the energy differences of the relaxed LE and ICT states of NMC6 and NTC6, as inferred from CC2 calculations with large TZVPP basis sets. At first, we shortly recall some results from previous work¹⁴ on DMABN. The gas-phase energetics of the LE \rightarrow ICT reaction were calculated at the CC2 level, and a slightly exothermic value ($\Delta E = -0.07$ eV) was found. However, from single-point calculations with more advanced coupled-cluster models it was concluded that CC2 tends to overestimate the stabilization of the ICT state by about 0.2 eV. A similar error is expected for the systems considered in this work, as DMABN, NMC6, and NTC6, from their electronic structure, are very similar systems.

From Figure 3 it can be seen that, at the CC2 level of theory,

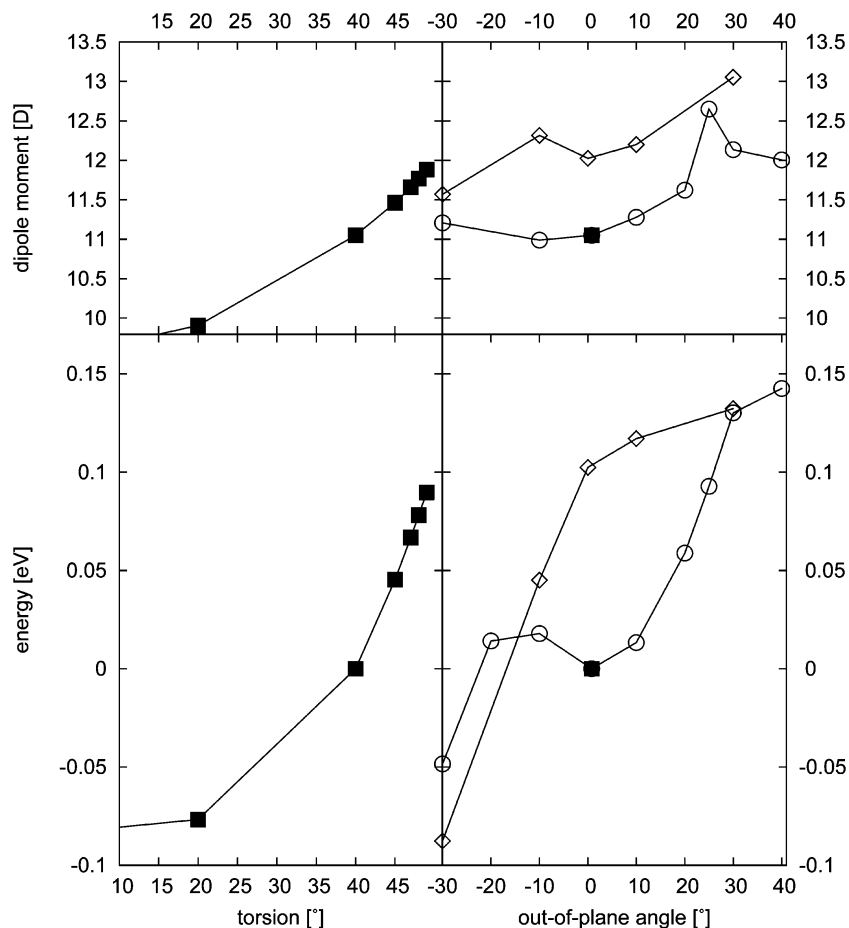


Figure 5. Minimum energy paths and corresponding dipole moments for the S_1 state of NMC6. On the left panels, the torsion angle of the amino group (nearly equivalent to the twist angle τ , see text) is held at fixed values while the remaining degrees of freedom were reoptimized. On the right panels, both torsion and out-of-plane angle ϕ_2 were held fixed (torsion of 40° (\circ); torsion of 50° (\diamond); the solid square is the (local) minimum that coincides with the left panel). The energy scale uses as reference point the local (LE-type) minimum at 40° .

the LE \rightarrow ICT reaction is only minimally exothermic for NMC6 ($\Delta E(\text{LE} \rightarrow \text{ICT-1}) = -0.01$ eV), and the more strongly polar ICT-2 and ICT-3 conformers lie at a significantly higher energy (+0.1 eV relative to ICT-1). Considering the estimate of higher-order correlation effects of +0.2 eV, the absence of dual fluorescence for this molecule is plausible. For NTC6, on the other hand, all ICT- n conformations lie about 0.2 eV below the LE state and thereby significantly lower than the ICT state in the comparable calculations on DMABN. Considering again the higher-order corrections for the LE/ICT energy difference, we estimate that both states, LE and ICT, have about the same energy in the gas phase. Indeed, dual fluorescence in NTC6 occurs (at difference to DMABN) already for rather nonpolar solvents.⁷ Above that, all ICT- n structures of NTC6 are more polar than their counterparts for NMC6. The barrier height (estimated to be below 0.1 eV in the preceding paragraph) will of course be increased by higher-order correlation effects, as well, depending on the amount of ICT character at the transition structure. Solvent effects, on the other hand, reduce the barrier height (again depending on the ICT character, as the solvation energy increases with the dipole moment). It appears thus plausible that in solution only a small barrier from the LE region toward the ICT region exists.

Remarkably, these differences between NMC6 and NTC6 are induced by a simple change of an alkyl group which does not directly interfere with the electronic π -system. As indicated in

the discussion of Figures 5 and 6, the main effect of a larger alkyl group is a *destabilization* of the LE state relative to the ICT state, because the bulky *tert*-butyl substituent enforces a strong twist of the amino group in the LE state and thereby weakens the stabilizing $n-\pi^*$ interactions. The ICT states of NMC6 and NTC6, on the other hand, have very similar structures; i.e., the influence of the alkyl-substituent is much smaller here. But still, the larger group causes a more planar amino group (see section 3.3) which leads to increased dipole moments in comparison to the case for NMC6 and lowers the energy difference between ICT-1 and the more polar ICT-3 conformation.

A hypothetical planar ICT structure, on the other hand, does not provide such an evident explanation why dual fluorescence is favored with increasing size of the substituent. Rather, a planar ICT state is expected to be as much destabilized as the LE state, and it is not clear why a change of the alkyl group should favor one or the other. The energy gap criterion remains valid, as can be seen from Figure 1: The calculated energy difference between S_1 and S_2 at the ground state geometries of, respectively, NMC6 and NTC6 is markedly smaller for NTC6. Thus the present calculations underline that this criterion and the TICT criterion of sufficient structural flexibility are independent of each other.

The finding that an ICT state with a strong twist ($>60^\circ$) is in principle possible for NTC6 (and even for NMC6, where it

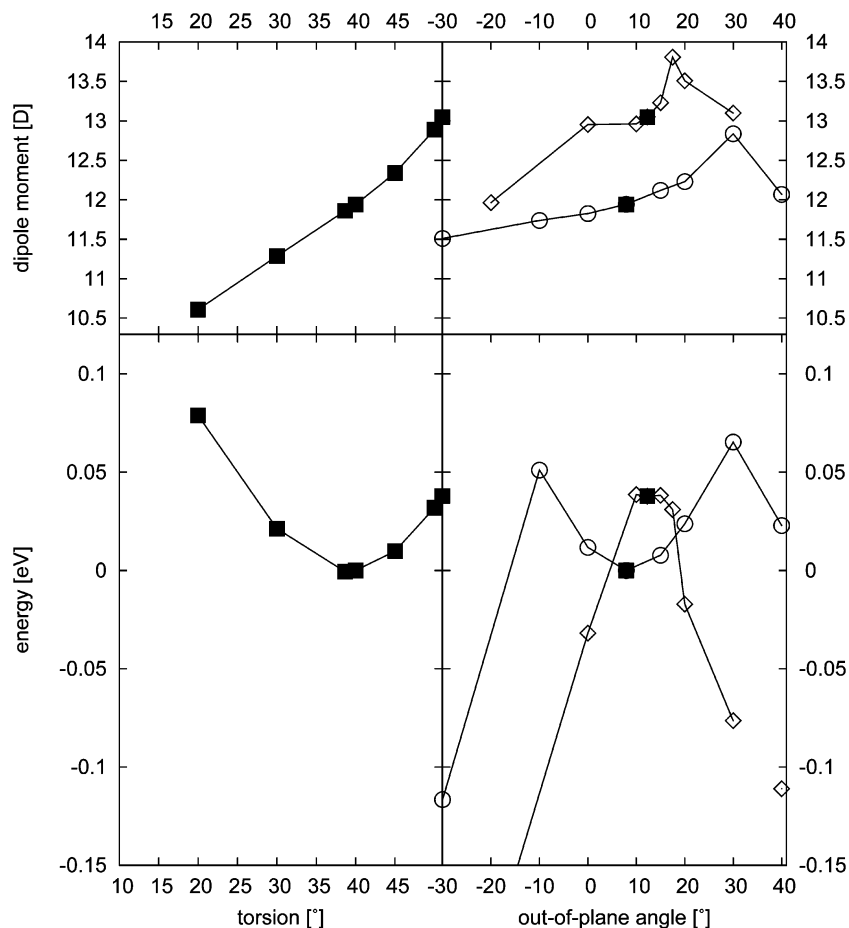


Figure 6. Minimum energy paths and corresponding dipole moments for the S_1 state of NTC6. For detail see caption of Figure 5. On the right panels, the points marked with \circ correspond to the 40° torsion angle, while those marked with \diamond correspond to the 51° torsion angle.

is energetically too high-lying to be populated in an $LE \rightarrow ICT$ equilibration process) gives support to the assumption that the mechanism for dual fluorescence in all alkylamino-benzonitriles is essentially the same. Recent gas-phase measurements of the short-time dynamics in DMABN derivatives after excitation to the L_a state^{43–46} indeed give a very similar pattern for all considered molecules, also for NMC6, ref 47. The authors interpret their results in favor of a temporary population of an ICT state shortly after L_a excitation (direct relaxation through a conical intersection on a time scale below 100 fs), and the anisotropy of the ion signal measured in that time window is ascribed to a resonant ionization due to a significant twist of the molecule ($>45^\circ$). Our calculation support the authors' assumption that such a strong twist is possible for NMC6. On the other hand, Gómez and co-workers⁴¹ have pointed out that the initial dynamics need not necessarily include the twist coordinate, as the minimum of the conical intersection seam (calculated at the CASSCF level) lies at 0° twist angle. The energy of the seam does not increase notably until around 30° – 40° twist angle in those calculations⁴¹ such that significant

branching of the trajectories toward ICT cannot be excluded.

The presence of a directly populated ICT state, however, was doubted on grounds of recent subpicosecond time-resolved excitation spectra of DMABN in *n*-hexane and acetonitrile.⁴⁸ It is argued that no ICT state absorption bands are present in the spectra recorded in *n*-hexane while changes in the LE-Band on the picosecond scale are attributed to solvent cooling. Yet, no alternative explanation for the short-time effects in the gas-phase measurements of Fuss and co-workers^{43,44} results from this assumption.⁴⁷ From spectra of DMABN recorded in acetonitrile,⁴⁸ in which already at delay times of 200 fs a band occurs which is attributed to the ICT state, it is concluded that no large amplitude motion takes place after this time (implicitly excluding a twisted conformation). However, a partial direct population of the ICT state through a conical intersection would not exclude a significant molecular distortion (such as a twist motion) in an ultrafast process. This cannot be ruled out on grounds of the *n*-hexane spectra of ref 48 as the position of the conical intersection (and thus the branching ratio between LE and ICT population) will depend on the solvent polarity.

As mentioned in the introduction, the assumption of a biradicalic ICT state is in conflict with the interpretation of a recent time-resolved X-ray experiment on crystalline DIABN.⁸

(42) Parusel, A. B. J.; Köhler, G.; Grimme, S. *J. Phys. Chem. A*, **1998**, *102*, 6297–6306.

(43) Fuss, W.; Pushpa, K. K.; Rettig, W.; Schmid, W. E.; Trushin, S. A. *Photochem. Photobiol. Sci.* **2002**, *1*, 255–262.

(44) Trushin, S. A.; Yatsuhashi, T.; Fuss, W.; Schmid, W. E. *Chem. Phys. Lett.* **2003**, *376*, 282–291.

(45) Yatsuhashi, T.; Trushin, S. A.; Fuss, W.; Rettig, W.; Schmid, W. E.; Zilberg, S. *Chem. Phys.* **2004**, *296*, 1–12.

(46) Fuss, W.; Rettig, W.; Schmid, W. E.; Trushin, S. A.; Yatsuhashi, T. *Faraday Discuss.* **2004**, *127*, 23–33.

(47) Fuss, W.; Schmid, W. E.; Pushpa, K. K.; Trushin, S. A.; Yatsuhashi, T. *Phys. Chem. Chem. Phys.*, submitted.

(48) Druzhinin, S. I.; Ernsting, N. P.; Kovalenko, S. A.; Lustres, L. W.; Senyushkina, T. A.; Zachariasse, K. A. *J. Phys. Chem. A*, **2006**, *110*, 2955–2969.

Although calculations support the assumption that an ICT state with lower energy than an LE state can be formed at low twist angles (see refs 14, 41) provided that substituent and/or environment effects tune the LE and ICT energies appropriately, the driving force for lowering the twist angle from 14° to 10° , as inferred from the experiment, is not evident from theory. The issue remains to be clarified in future work.

At this point we recall that conclusions made in the present work apply to alkylamino-benzonitriles only, as stated in the introduction. Dual fluorescence from a planar ICT state was indeed observed⁹ for fluorazene (abbreviated FPP), a derivative of *N*-phenylpyrrole (PP) in which the rotation about the single bond between the phenyl and pyrrolo groups is rigidized by a methylene bridge. The near-planarity of the ICT state was recently confirmed theoretically.⁴⁹ Although not explicitly noted by the authors of ref 49, there is an important difference to ICT in amino-benzonitriles: The ICT process in FPP involves a different orbital on the donor, i.e., the highest π -orbital of pyrrole. This orbital does not include the nitrogen lone pair and thus is not present in the case of amino-benzonitriles. Further excited states exist for PP and FPP which involve the nitrogen lone pair and which thus are equivalent to the excited states of amino-benzonitriles (see ref 50). For the flexible PP therefore both planar and twisted ICT states are accessible.⁴⁹

4. Conclusions

We have carried out quantum-chemical calculations on the excited states of the alkyl-aminobenzonitrile derivatives NMC6 and NTC6. Our structure optimizations show that the molecular systems are flexible enough to allow for a twist of the amino group of up to 69° . From our calculations, it therefore follows that the situation is essentially the same as the one established for DMABN; i.e., the ICT state is of biradicalic nature, and a twist of the amino group leads to an energetically low-lying region of the energy surface from where fluorescence can occur.

Concerning the LE state of NTC6, our calculations suggest that it is more strongly polar than that of NMC6 and NIC6, and fluorescence from this state will therefore show a larger

solvatochromic shift than that observed for the other two molecules. The reaction path toward the ICT region of the excited-state hypersurface involves the amino-group twist, the pyramidalization of the ring carbon atom to which the amino group connects, and a change in the bond pattern of the phenyl moiety from a Kekulé-like arrangement to a quinoid form. The barrier of the equilibration reaction is calculated to be sufficiently small to be overcome under experimental conditions.

The results offer a consistent explanation why NTC6 is dually fluorescent while NMC6 is not. The key is a *destabilization* of the LE state by large substituents which enforces a twisted amino group and thereby reduces the $n-\pi^*$ interaction of the amino group and phenyl moiety. The structures of the twisted ICT state, on the other hand, remain nearly independent of the size of the alkyl group. In contrast to that the substituent effects are not consistent with a planar ICT state, as they do not explain why a larger alkyl group should energetically favor the ICT state, as compared to an LE state that is preferably planar as well. This argument, which is actually independent of our calculations, provides indirect evidence against such an ICT structure.

The main finding of our work—the increased flexibility of aromatic groups in the excited-state which allows for structures that cannot be predicted from rules applying to the ground state only—may also play a role for other photochemically interesting systems. This underlines the importance of advanced quantum-chemical model calculations for the prediction and understanding of excited-state structures.

Acknowledgment. This work was supported by the Deutsche Forschungsgemeinschaft through Project HA2588. One of the authors (A.K.) is grateful for a fellowship financed by the Deutsche Forschungsgemeinschaft (KO2337). We thank Dr. Fuss (TU München) for valuable discussions and for providing a preprint of ref 47.

Supporting Information Available: ASCII file with Cartesian coordinates of all considered structures. PDF file with details on the Onsager model. This material is available free of charge via the Internet at <http://pubs.acs.org>.

JA0642010

(49) Xu, X.; Cao, Z.; Zhang, Q. *J. Phys. Chem. A* **2006**, *110*, 1740–1748.
(50) Cogan, S.; Zilberg, S.; Haas, Y. *J. Am. Chem. Soc.* **2006**, *128*, 3335–3345.